Self-Assembly of Cetyl Linear Polyethylenimine To Give Micelles, Vesicles, and Dense Nanoparticles

Wei Wang, Xiaozhong Qu, Alexander I. Gray, Laurence Tetley, and Ijeoma F. Uchegbu*

Department of Pharmaceutical Sciences, University of Strathclyde, 27 Taylor St, Glasgow G4 0NR, U.K., and Electron Microscopy Unit, Institute of Biomedical and Life Sciences, University of Glasgow G12 8QQ, U.K.

Received May 14, 2004; Revised Manuscript Received September 8, 2004

ABSTRACT: The involvement of macromolecules in the formation of biological and other membranes has important implications for structural biology and nanoengineering. Using cetyl polyethylenimines of varying molecular weight and hydrophobicity, it was found that polymer hydrophobicity (mol % cetylation) controlled the nature of the self-assembly, giving micellar (cetyl groups < 23 mol %), vesicular (cetyl groups = 23−42 mol % or cetyl groups = 3−42 mol % with cholesterol), and dense nanoparticle (cetyl groups ≥ 49 mol %) aggregates. Thick (up to 15 nm) membranes due to the polyelectrolyte coating with the amphiphile were observed with low levels of cetylation only, and both d*n*/d*c* (indirectly) and vesicle/nanoparticle size (directly) varied linearly with mol % cetylation (r = 0.96−0.99).

Introduction

The key drivers for the structural arrangement of amphiphilic biomacromolecules in biological membranes and other biological colloids such as chylomicrons have received very little attention, with most studies focusing principally on the contribution made by lipids.[1] A clearer understanding of macromolecular amphiphile self-assembly into membranes is thus required. Furthermore, an appreciation of the link between macromolecular architecture and macromolecular self-assembly[2−4] may lead to the development of new nanosystems/nanomachines with potential applications in a number of fields. Soluble polymers with various hydrophobic and/or hydrophilic grafts[2−4] are excellent model compounds for the study of macromolecular self-assembly. Lower levels of hydrophobicity in poly(amino acid) polymers bearing hydrophobic grafts (less than 45 mol % of the monomer units hydrophobized) and a reduced degree of polymerization result in the formation of bilayer membranes[4] while higher levels of hydrophobic grafting result in the production of solid nanoparticles.[2] There is also a direct relationship between carbohydrate amphiphile polymer radius of curvature (vesicle mean size) and degree of polymerization.[3] In an effort to specifically characterize the influence of hydrophobicity on macromolecular self-assembly and the influence of polymerization per se on the same, we have studied the self-assembly of amphiphiles prepared from linear polyethylenimine (LPEI) which is available as a low molecular weight (LMW) compound (M_n = 423 Da) and as a polymer (M_w = 25 000 Da). More specifically, although high molecular weight LPEI[5] (MW = 22 000 Da) and its LMW (M_n = 423 Da) cholesteryl amphiphile[6] have found applications as gene delivery tools, information on the self-assembly of LPEI amphiphiles is unavailable. Branched polyethylenimine (PEI) amphiphiles, on the other hand, while also recently tested as gene delivery systems[7,8] are known to aggregate into micelles,[9−12] accumulate at the oil/water interphase of oil in water emulsions,[11] and be incorporated into phospholipid vesicle membranes.[13,14]

Scheme 1. Synthesis of HCPEI and LCPEI

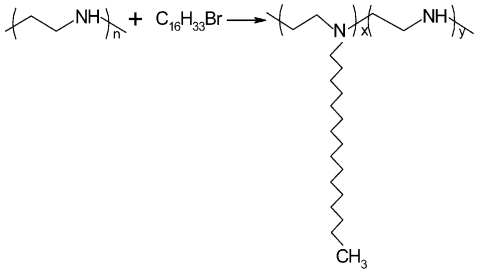

Providing information on the key drivers for macromolecular amphiphile self-assembly into micelles, vesicles, or solid nanoparticles is the aim of this study. Such information may lead to a further understanding of the structural participation of macromolecules in the formation of biomembranes/biocolloids and also provide a background for the development of new nanosystems with superior functionalities.

Materials and Methods

Materials. High molecular weight (HMW) LPEI (M_w = 25 000 Da, M_n = 10 000 Da) was purchased from Polysciences Inc., Germany. LMW LPEI (M_n = 423 Da), 1-bromohexadecane, tetrahydrofuran (THF), triethylamine (TEA), methyl orange, deuterated solvents, sodium bicarbonate, sodium tetraborate decahydrate, and Dowex M-43 ion-exchange resin were all obtained from Sigma-Aldrich, UK. All other organic solvents were purchased from Merck UK. Nanovan (methylamine vanadate) was obtained from Nanoprobes Inc. All chemicals were used without further purification.

Preparation of HMW Cetyl LPEI (HCPEI). This was carried out as shown in Scheme 1. Three methods were used as detailed below.

Absolute Alcohol as Medium. Sodium hydroxide (0.5 g) was dissolved in absolute alcohol (20 mL) in a round-bottom flask, and to this was dissolved PEI (0.5 g). An amount of 1-bromohexadecane (Table 1) was then added, and the reaction mixture was refluxed for 24 h. The reaction mixture and the reaction flask rinsings (water, 50 mL) were exhaustively dialyzed (molecular weight cutoff = 12 000−14 000 Da) against

* Corresponding author: e-mail i.f.uchegbu@strath.ac.uk.

10.1021/ma049042o CCC: $27.50
Published on Web 10/27/2004

Table 1. Synthesis of PEI Amphiphiles

samples	synthesis solvent	initial CH_2CH_2N-, CH_3-$(CH_2)_{15}$-Br molar ratio	yield (%)	level of cetylation (%)[a], (no. of cetyl chains per molecule)	d*n*/d*c* (mL g^{-1})	solvent for d*n*/d*c*	M_w (kDa)	T_{m1}, T_{m2}[b] (°C)
HCPEI 1	ethanol	1:0.05	98	1 (2.4)	0.204	ethanol	28	62
HCPEI 2	ethanol	1:0.15	101	2 (4.8)	0.202	ethanol		
HCPEI 3	ethanol	1:0.25	105	3 (7.1)	0.196	ethanol	30	60
HCPEI 4	ethanol	1:0.35	106	4 (9.5)	0.188	ethanol	31	51
HCPEI 8	chloroform	1:0.03	71	8 (19)	0.174	ethanol	33	
HCPEI 18	chloroform	1:0.08	75	18 (42)	0.105	chloroform	53	28, none
HCPEI 23	chloroform	1:0.15	77	23 (55)	0.100	chloroform	54	28, none
HCPEI 33	chloroform	1:0.25	80	33 (79)	0.088	chloroform	63	28, none
HCPEI 49	chloroform	1:0.35	85	49 (117)	0.062	chloroform	72	
HCPEI 68	chloroform	1:0.50	88	68 (162)	0.033	chloroform	96	28, none
LCPEI 14	chloroform	1:0.13	52	14 (1.4)		ethanol	0.74[c]	
LCPEI 23	chloroform	1:0.25	58	23 (2.3)			0.87[c]	
LCPEI 42	chloroform	1:0.49	73	42 (4.2)		ethanol	1.32[c]	
HCPEI 24	tetrahydrofuran	1:0.10	70	24 (57)	0.098	chloroform	58	
HCPEI 37	tetrahydrofuran	1:0.20	73	37 (88)	0.080	chloroform	64	28, none
HCPEI 96	tetrahydrofuran	1:0.70	90	96 (229)	0.011	chloroform	120	31, 62

[a] Level of cetylation (%) = moles of cetyl groups per 100 mol of ethylenimine units. [b] T_{m1} = first phase transition temperature, T_{m2} = second phase transition temperature. [c] Calculated from cetylation levels.

distilled water (5 L with 6 changes over 24 h). The dialysate was subsequently freeze-dried, washed with diethyl ether (3 × 50 mL), dried, and collected as a white powder.

Chloroform as Medium. PEI (0.5 g) was dissolved in chloroform (20 mL), and to this solution was added TEA (0.5 mL) and an amount of 1-bromohexadecane (Table 1). The solution was refluxed for 24 h, then first dialyzed (molecular weight cutoff = 12 000−14 000 Da) against 40% v/v ethanol (5 L), and subsequently dialyzed against distilled water (5 L with 6 changes over 24 h). The dialysate was finally freeze-dried and collected as a light yellow solid.

THF as Medium. PEI (0.5 g) was dissolved in THF (10 mL). To this THF solution was added NaOH (0.5 g) dissolved in methanol (10 mL) and an amount of 1-bromohexadecane (Table 1). The solution was refluxed for 48 h, dialyzed as described under "Chlorofom as Medium", and freeze-dried to give a light yellow solid.

Preparation of LMW Cetyl LPEI (LCPEI). PEI (2 g) was dissolved in chloroform (20 mL), and to this was added an amount of 1-bromohexadecane (Table 1). The solution was refluxed for 24 h and evaporated under reduced pressure, and the residue washed with diethyl ether and dried. Samples containing a high level of cetylation (e.g., LCPEI 42) were dissolved in methanol and centrifuged (1000*g* × 30 min, Heraeus Biofuge), and the supernatant was evaporated to dryness. The dried product was then dissolved in absolute ethanol (100 mL) and passed through a Dowex M43 column (500 mm × 40 mm). Prior to chromatography the column was washed with absolute alcohol (3 × 50 mL). The clear eluate was then evaporated to dryness and the product obtained as a yellow semisolid or yellow solid. In some cases an alternative purification method was chosen for samples which still had high levels of bromide ions after passage through the resin. These latter LCPEIs were exhaustively dialyzed (molecular weight cutoff = 1350 Da) against water (5 L).

Structural Characterization. *^{1}H NMR Analysis.* ^{1}H NMR with ^{1}H correlation experiments were performed on solutions of HCPEI and LCPEI dissolved in deuterated methanol or deuterated chloroform using a Bruker AMX 400 MHz spectrometer (Bruker Instruments, UK) and a temperature of either 45 or 50 °C.

Elemental Analysis. An analysis for C, H, and N was performed using a Perkin-Elmer 2400 analyzer. Bromide content was analyzed using a mercuric nitrate titrimetric method with diphenylcarbazone as indicator.

Laser Light Scattering. The molecular weights of LPEI and HCPEI samples were measured in microbatch mode using a DAWN EOS laser light scattering instrument (λ = 690 nm, Wyatt Technology) and either ethanol or chloroform (HPLC grade) as solvent. A Rheodyne 7725 sample injector was used to load the filtered (0.2 or 0.45 μm) samples onto the instrument, and the molecular weights were obtained from Zimm plots processed using Astra for Window 4.73 software.

Static light scattering measures the angular dependence of the excess Rayleigh ratio $R(\theta)$ (light scattering of the solution as a function of the scattering angle θ which is proportional to the scattering due to the dispersed molecules, i.e., in excess of that due to the solvent), and such data may be used to calculate the mean-square radius or radius of gyration (r_g), the second virial coefficient A_2, and the weight-average molar mass (M_w) using eq 1 as derived from the early studies of Zimm.[15,16]

$$\frac{K^*c}{R(\theta)} = \frac{1}{M_w}\left[1 + \frac{16\pi^2}{3\lambda_0^2}\langle r_g^2\rangle \sin^2(\theta/2)\right] + 2A^2c \qquad (1)$$

where $K^* = [4\pi^2 n_0^2 (dn/dc)^2]/(N_A\lambda_0^4)$, $R(\theta)$ is the excess Rayleigh ratio, n_0 is the solvent refractive index, d*n*/d*c* is the specific refractive index increment, N_A is Avogadro's number, λ_0 is the wavelength of the incident beam in vacuo, θ is the scattering angle, and M_w is the weight-average molar mass. Zimm plots of $K^*c/R(\theta)$ vs $\sin^2(\theta/2) + kc$ (where k is a scaling factor with units of inverse concentration) can be used to measure the molar mass of polymers/polymer aggregates as an extrapolation to a scattering angle of 0°, and a concentration of zero yields an intercept equivalent to $1/M_w$.

Refractive index increments (d*n*/d*c*) of the above polymer solutions in their respective solvents were measured with an OPTILAB DSP interferometric refractometer (Wyatt Technology, λ = 690 nm) at 25 °C. Once again a Rheodyne 7725 sample injector was also used to load the filtered (0.2 or 0.45 μm) solutions on to the instrument, and the data were processed using DNDC for Windows 5.31 software.

Differential Scanning Calorimetry (DSC). DSC scans were performed with Mettler Toledo DSC 30 (Mettler Toledo, UK). Polymer samples (7.3 mg) were sealed in 40 μL standard aluminum crucibles and were scanned at a heating rate of 5 °C min^{-1}.

Polymer Self-Assembly. *Preparation of HCPEI and LCPEI Supramolecular Structures.* HCPEI or LCPEI samples (4−20 mg mL^{-1}) were dispersed in distilled water by probe sonication (10−30 min to obtain a visually homogeneous dispersion) using a Soniprep 150 probe sonicator (SANYO, MSE) with the instrument set at its maximum output. Samples were then filtered (0.45 μm). In some cases a quantity of cholesterol equivalent to between 10 and 50% of the weight of the polymer was added prior to probe sonication.

Sizing of Supramolecular Structures. Colloid particle size was measured by photon correlation spectroscopy (PCS) (Malvern Zetasizer 3000 HS) at 25 °C. Measurements were performed in triplicate. PCS measures the particle diffusion

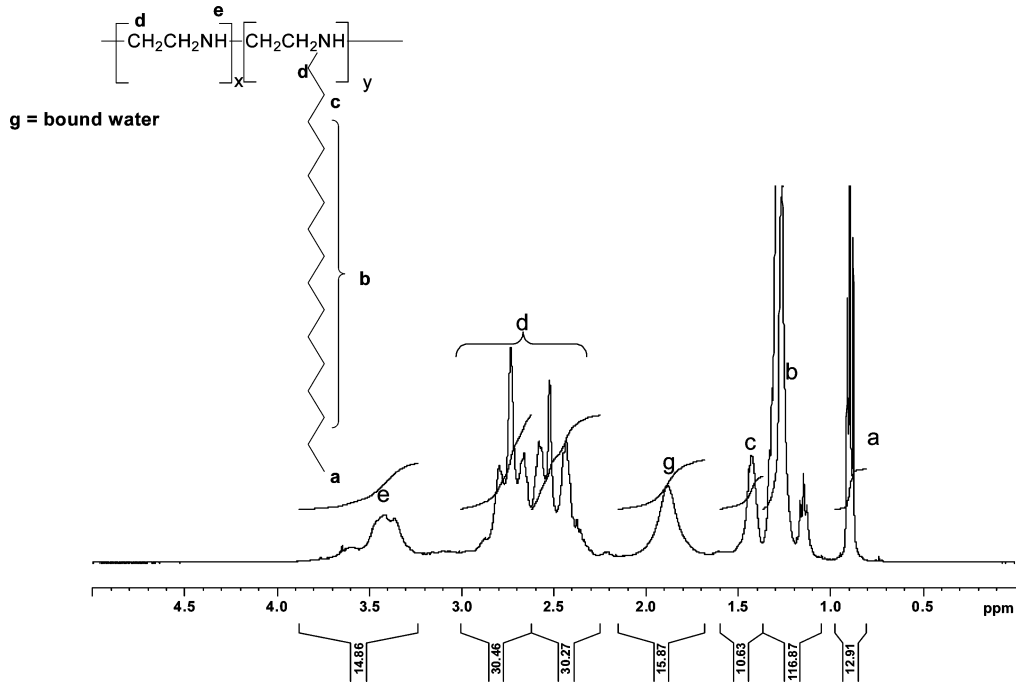

Figure 1. ^{1}H NMR of HCPEI 24 (24 mol % cetylation) in $CDCl_3$.

coefficient D and converts this to the hydrodynamic diameter (D_h) using the Stokes−Einstein equation:[17]

$$D_h = 2R_h = kT/3\pi\eta D \quad (2)$$

where R_h is hydrodynamic radius, k is the Boltzmann constant, T is absolute temperature, and η is the solvent viscosity.

Electron Microscopy. Negative stained and freeze-fracture transmission electron microscopy were carried out as previously described[3,4] using a LEO 912AB OMEGA energy filtering electron microscope (Carl Zeiss, Germany).

Differential Scanning Calorimetry. Supramolecular dispersions (100 μL) in water were sealed in 120 μL stainless steel medium-pressure DSC crucibles and were scanned against an equal volume of pure water at a heating rate of 2 °C min^{-1}.

UV−Vis Spectrophotometry. LCPEI samples were dispersed in a solution of methyl orange (25 μM) in borate buffer (0.02 M, pH 9.4) by probe sonication as detailed above. Dispersions were incubated for 1 h at room temperature, and their UV absorption spectrum was recorded (300−600 nm) on a Unicam UV 300 spectrophotometer (Thermo-Spectronic, UK).

Laser Light Scattering. A DAWN EOS static laser light scattering instrument (Wyatt Technology) was used to analyze the vesicles formed in water using distilled water as the disperse phase. A Rheodyne 7725 sample injector was used for loading different concentrations of the filtered (0.45 μm) dispersions. The M_w, R_g, and A_2 of the vesicles were obtained from Zimm plots processed using Astra for Windows 4.73 software (Micro-Batch Mode). Refractive index increments (dn/dc) of the colloidal dispersion in water were measured as described above, except that colloidal dispersions were filtered using a 0.45 μm filter.

Results and Discussion

Synthesis of HCPEI and LCPEI. The synthesis of the amphiphiles was confirmed by NMR (e.g., Figure 1). Proton assignments for HCPEIs are given in Figure 1. The signal at 1.14 ppm originates from a minor solvent contaminant. Proton assignments for LCPEIs were as follows: δ 0.88 ppm = CH_3−C (cetyl), δ 1.26 ppm = CH_2−C (cetyl), δ 1.41 ppm = CH_2−C (cetyl), δ 2.17−3.02 ppm = CH_2−N (cetyl, PEI). While previously we have used proton NMR to estimate the level of grafting of water-soluble polymers with hydrophobic and hydrophilic grafts,[2,4,18] the overlapping of the cetyl and PEI CH_2N peaks prevents the application of NMR in this case. The levels of cetylation were thus determined using elemental analysis.

Table 1 gives details of the polymer yields (calculated as a % of the starting polymer weight) and the mol % cetylation (moles of cetyl groups per 100 ethylenimine units) levels. Polymers are labeled with a suffix number representing the mol % cetylation of the polymer. Table 1 shows that as the hydrophobicity of the synthesis media increased, the speed of the reaction and hence the level of alkylation increased. Hence, a judicious choice of reaction solvents and LPEI and 1-bromohexadecane feed ratios resulted in a series of polymers with various levels of alkylation (Table 1). A qualitative analysis of the HCPEIs (~10 mg mL^{-1}) solubilities in methanol, ethanol, chloroform, and diethyl ether revealed that HCPEIs with less than 8 mol % cetylation were only soluble in methanol and ethanol, while HCPEIs with between 18 and 33 mol % cetylation were only soluble in ethanol, chloroform, and diethyl ether, and a cetylation level in excess of 37% conferred solubility in only chloroform and diethyl ether. These observations are in keeping with the behavior of a series of alkylated polyelectrolytes with increasing hydrophobicity. The starting material (HMW LPEI) is only soluble in methanol, ethanol, and chloroform (manufacturer's data). The purification of the HCPEIs involved either (a) washing with diethyl ether prior to dialysis against water (polymers with less than 4 mol % cetylation) or (b) dialysis against 40% v/v ethanol (all other polymers). The higher than expected cetylation levels with some HCPEIs (e.g., HCPEI 96) is a result of the loss of polymer chains with lower levels of cetylation on dialysis (12 000−14 000 Da molecular weight cutoff) against 40% v/v ethanol. Such loss is favored by (a) the polydispersity of the starting polymer (M_n = 10 000 Da), (b) limited coil expansion of lightly substituted HCPEI in ethanol−water, and (c) aggregation of the highly alkylated chains in ethanol−water. Furthermore, residual hydration (Figure 1) would increase the overall

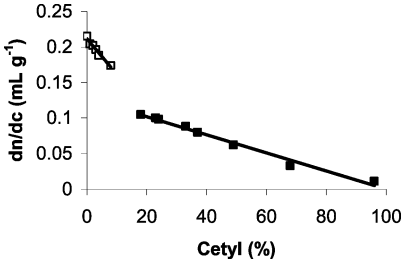

Figure 2. Influence of cetylation levels on dn/dc (λ = 690 nm): □, determinations in ethanol; ■, determinations in chloroform.

yield value. Traces of bromide were detected in HCPEI 3 (0.81% w/w) and HCPEI 33 (0.43% w/w) only. The M_w of HCPEIs increased with increasing levels of cetylation (Table 1).

Three different LCPEIs were synthesized (Table 1) with all containing residual levels of bromide (0.9, 1.64−2.56, and 1.80% w/w for LCPEI 23, LCPEI 14, and LCPEI 42, respectively).

Further evidence of the production of the various cetylated linear PEIs is given by the decrease in dn/dc with increasing levels of cetylation (Figure 2), evidence of the decreasing polarizability of the polymer. A decrease in dn/dc is also observed with increasing acetylation of chitosans.[19] As fatty alkyl chains substitute ethylenimine units in each unit of molar mass, the polarizability of the polymer in each unit of mass would be expected to decrease. However, interestingly perfect linear relationships were observed for dn/dc values (recorded within the same solvent) and the mol % cetylation. The equation of the straight line is given by eqs 3 and 4:

$$\mathrm{d}n/\mathrm{d}c = -0.0013Ct + 0.1271 \ (r = 0.995) \quad \text{(for determinations in chloroform)} \quad (3)$$

$$\mathrm{d}n/\mathrm{d}c = -0.0049Ct + 0.2113 \ (r = 0.98) \quad \text{(for determinations in methanol)} \quad (4)$$

where Ct = mol % cetylation. dn/dc measurements may thus be used to determine the level of hydrophobic modification of synthetic polymers or the lipid content of biopolymers. The value of the slope of the straight line is a reflection of the contribution of the solvent to the polarizability of the solution as the dielectric constants of chloroform and ethanol at 20 and 25 °C are 4.8 and 24.3, respectively, thus explaining the steeper slope obtained with ethanol when compared to chloroform.

DSC analysis on the HCPEIs revealed between one and two thermal phase transitions (Table 1, Figure 3). HMW linear PEI is a solid at room temperature with a melting point of 76 °C (data not shown). At low (1−4 mol %) levels of cetylation (Figure 3, only data for HCPEI 1 is shown), the cetyl chain melting endotherms at the lower temperature of 28 °C are barely observed, and only the high-temperature signal for the melting of the polymer main chain is observed. The signal for the melting of the polymer main chain disappears as cetylation levels increase to 18% (HCPEI 18, Figure 3) due to interference in the ordered main chain packing by the cetyl chains. As cetylation levels increase to 68 mol % (HCPEI 68, Figure 3), there are also no observable transitions due to the main PEI chains. Finally at the highest cetylation levels, separate cetyl melting endotherms and main chain melting endotherms are observed, and the cetyl groups because of their abundance are seen to make a contribution to the main chain melting endotherm (HCPEI 96, Figure 3). The DSC data are further evidence of the synthesis of the amphiphiles. Alkylated branched 25 000 Da PEIs are also either viscous liquids or solids with increasing levels of alkylation and exhibit a melting endotherm at about 20 °C with alkylation levels of about 20%.[11]

LCPEI and HCPEI Self-Assembly. *LCPEI.* LMW cetyl PEI was chosen for the study as cetyl derivatives of this molecule may be used to effectively represent low molecular weight amphiphiles as even when up to four of the ethylenimine nitrogens are cetylated the molecular weight is still in the region of 1000 Da (Table 1). For example, the molecular weight of the membrane

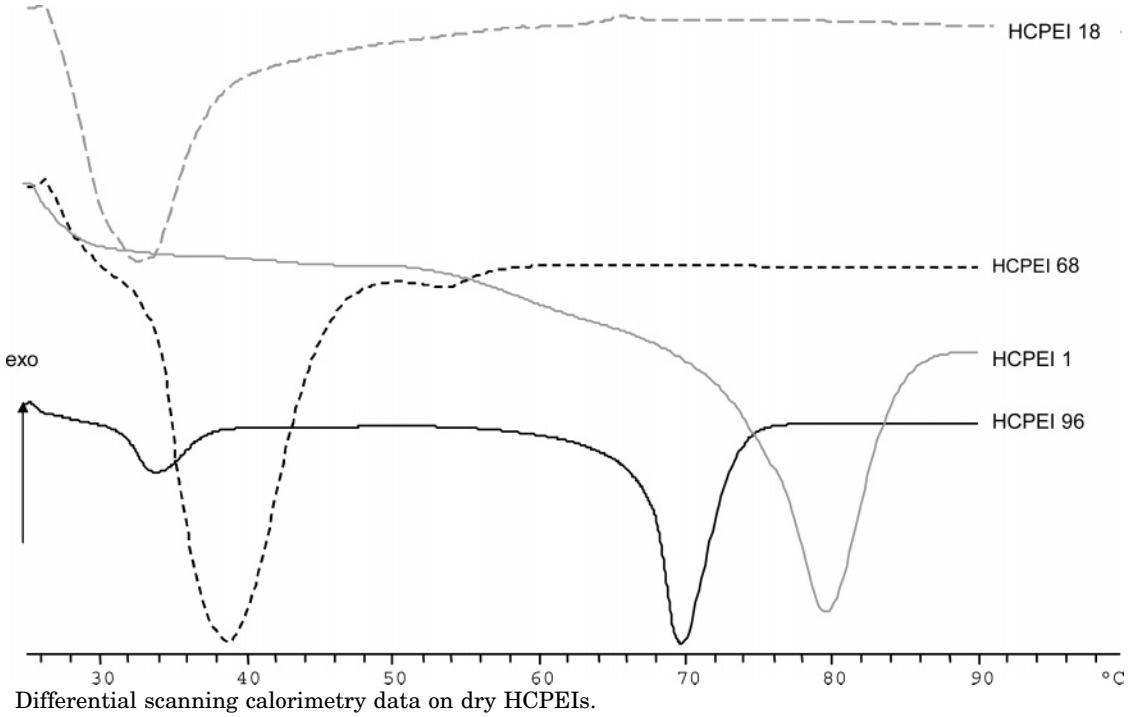

Figure 3. Differential scanning calorimetry data on dry HCPEIs.

forming phospholipid dipalmitoylphosphatidylcholine is 734. The change in the wavelength of maximum absorbance in the methyl orange spectrum was used to monitor aggregation of the amphiphiles.[20,21] The aggregation of LCPEI molecules (Figure 4a) results in micelles and larger nanoparticles (Figure 4b). The % hydrophobic content of these amphiphiles was estimated as that proportion of the molecule consisting of the distal 14 carbons that make up the hydrophobic chains (carbons bearing protons which are further upfield in the NMR spectra). Up to 45% hydrophobic content (2 cetyl chains per molecule) resulted in the formation of micellar aggregates while increasing the molecule's hydrophobic content to 60% (4 cetyl chains per molecule) resulted in the production of larger flat and spherical nanostructures (Figure 4b,c). Stabilization of the edges of these structures with areas of unsubstituted (hydrophilic) polymer is envisaged. The nanostructures consist of ordered arrays of amphiphile as differential scanning calorimetry analysis revealed the LCPEI 42 self-assemblies to have a phase transition temperature of 25 °C. The presence of a phase transition endotherm with these self-assemblies is evidence of the ordering of the alkyl side chains. Solid nanoparticles prepared from highly cetylated HCPEIs (see below) do not exhibit a phase transition temperature. However, while these flattened nanostructures (Figure 4c) are novel, their exact nature is at present unclear and warrants further study.

HCPEI Alone. The probe sonication of dispersions of the more hydrophilic HCPEIs (HCPEIs with less than 8 mol % cetylation; HCPEIs 1, 2, 3, 4, 8) at a concentration range of 4−20 mg mL^{-1} results in unstable micellar aggregates which quickly precipitate on cooling the probe sonicated dispersion. As the cetylation level rises to 18 mol %, tubular micelles of 42 nm in length are produced on probe sonication (Figure 5a). The unstained lipid interior of these structures (4 nm thick) leads us to conclude that these are micellar aggregates. The tubular nature of the micelles is evidence of the heterogeneity of the polymers; with polymers with a small angle of curvature (more hydrophobic) forming the axis of the tubules and polymers with a wider angle of curvature (more hydrophilic) stabilizing the ends of the close tubules. Thus, a minimum level of cetylation for the self-assembly of HCPEIs is 18 mol %. A higher level of cetylaton (23−37 mol %) leads to the production of flattened vesicular assemblies (Figure 5b); there is a subtle crossover point from micellar to vesicular assemblies of between 18 and 23 mol % cetylation or a hydrophobic content of 43−48%, and this is similar to the crossover point from micelles to nanostructures (45% hydrophobic content) observed with LCPEIs as detailed above. We can thus conclude that a hydrophobic content of more than 43−45% in linear PEIs prevents the formation of micellar assemblies irrespective of molecular weight. The phase transition temperatures recorded for HCPEI 24, 33, and 37 self-assemblies ranged from 39 to 40 °C. The flattened vesicular assemblies are further evidence of the heterogeneity of the polymers, and once again the more hydrophilic (less substituted) polymers are believed to stabilize the edges of the flattened species. The more hydrophobic HCPEIs with a cetylation level in excess of 37 mol % (HCPEIs 49, 68, and 96) produce particles that resist the ingress of the heavy metal stain and appear as solid spheres (Figure 5c). Hence, molecules containing 58% hydrophobic

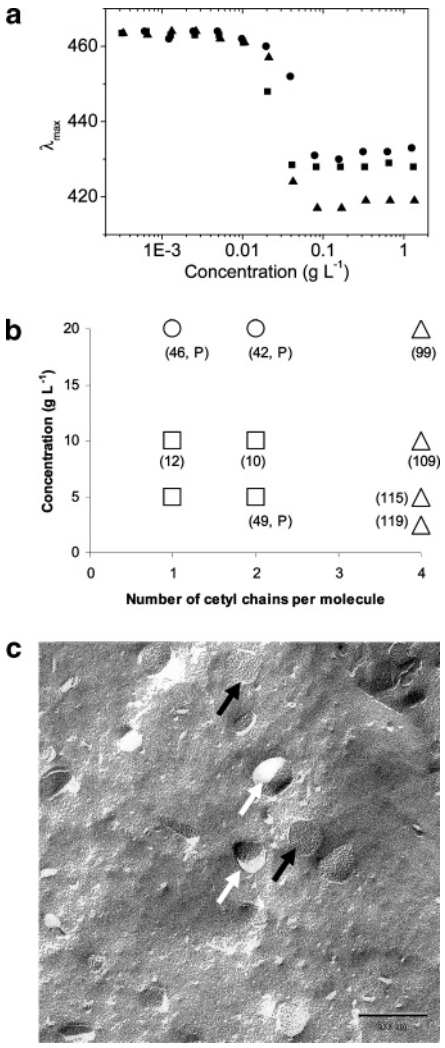

Figure 4. (a) Aggregation of LCPEIs (●, LCPEI 14−14 mol % cetylation; ■, LCPEI 23−23 mol % cetylation; ▲, LCPEI 42−42 mol % cetylation) as shown by the hypsochromic shift of methyl orange. The cmc values were recorded as 0.019, 0.013, and 0.018 g L^{-1} for LCPEI 14, LCPEI 23, and LCPEI 42, respectively. (b) Partial phase diagram for LCPEI aggregates on probe sonication in water: □, micellar dispersions; ○, unstable dispersions which phase separated (sedimented) within 4 h; △, cloudy particulate dispersions. Numbers in brackets give *z*-average mean particle sizes of the various dispersions (nm). *P* = polydisperse size distribution. (c) Freeze fracture electron microscopy micrograph of LCPEI 42 (42 mol % cetylation) particles (4 mg mL^{-1}) produced by probe sonication in water. Flat particles (absence of shadowing) are arrowed with black arrows while the more spherical structures (presence of shadowing) are arrowed with white arrows, bar = 200 nm.

content are no longer able to form bilayer vesicles, and solid nanoparticles are instead formed. These solid nanoparticles do not show a phase transition endotherm at the scanning temperature range of 25−85 °C. They are devoid of a phase in which the alkyl chains are ordered and are solid nanoparticles of an amorphous nature. In a manner similar to the LCPEIs, increasing polymer hydrophobicity produces micellar aggregates (18 mol % cetyl groups), vesicles (23−37 mol % cetyl groups), and solid nanoparticles (>37 mol % cetyl groups). Hence, membrane formation is observed at a hydrophobic content of between 43 and 58%. The current data are remarkably similar to earlier studies on poly-L-lysine vesicles where a level of hydrophobic

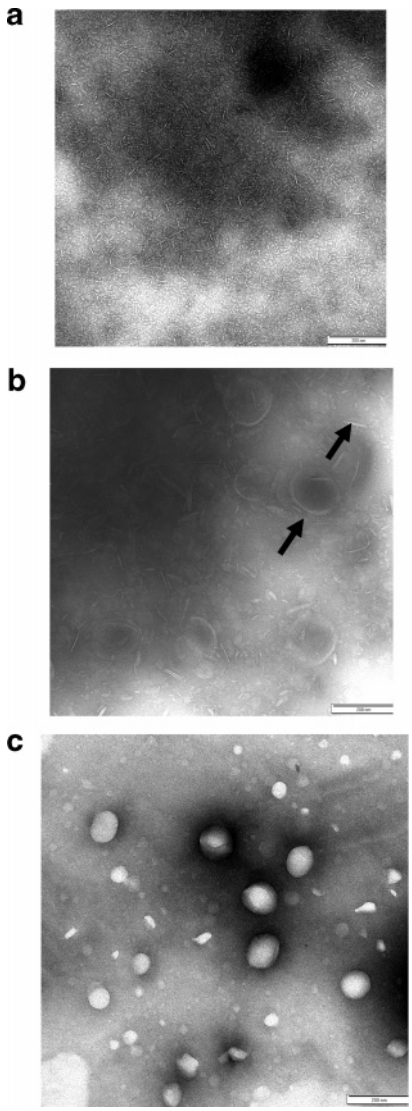

Figure 5. (a) Negative stained TEM of an aqueous dispersion (20 mg mL^{-1}) of HCPEI 18 (18 mol % cetylation) on probe sonication in water, bar = 200 nm. (b) Negative stained TEM of an aqueous dispersion (20 mg mL^{-1}) of HCPEI 33 (33 mol % cetylation) on probe sonication in water, bar = 200 nm. Flattened bilayer (side and top views are arrowed) particles are seen. (c) Negative stained transmission electron micrograph of a dispersion of HCPEI 49 (49 mol % cetylation) on probe sonication in water, showing dense nanoparticles (4 mg mL^{-1}), bar = 200 nm.

modification in excess of 45 mol % prevented the formation of vesicles.[24]

LCPEI, Cholesterol Dispersions. The membrane stabilizing agent cholesterol is known to improve the hydrophobic attractions[22,23] between the hydrophobic chains of amphiphiles, and bilayer vesicles were obtained with LCPEI 42 and cholesterol (Figure 6a). Differential scanning calorimetry revealed a phase transition temperature of 20 °C, a lower temperature than that recorded in the absence of cholesterol (25 °C). Cholesterol thus increases the fluidity of the polymer alkyl chains by integrating between them. Zimm plots[15,16] (Figure 6b) on the LCPEI, cholesterol aggregates produced M_w, R_g, and A_2 data, while photon correlation spectroscopy data[17] may be used to compute vesicle mean hydrodynamic radius (R_h). The ratio of R_g/R_h approximates 1.25 for all samples, an indication of the presence of prolate ellipsoid structures as seen in Figure 6a. An R_g/R_h value of 0.75 is expected for hard spheres. Ellipsoid bilayer vesicles are obtained in the case of cholesterol-containing samples and less well understood nanostructures when LCPEI 42 alone is dispersed in aqueous media.

The LCPEI aggregation number (N) of these vesicles/aggregates was calculated by using eq 5. An assumption is made that both LCPEI and cholesterol are fully associated with the particles. Indeed, no sediment was seen in the particle dispersion, although the presence of nonassociated water-soluble LCPEIs with low levels of cetylation cannot be ruled out.

$$N = x_1\left(\frac{M_w}{x_1 M_{w1} + x_2 M_{w2}}\right) \tag{5}$$

where M_w is the weight-average molecular weight of the aggregates, x_1 and x_2 the molar fractions of LCPEI and cholesterol in the dispersion, and $x_1 + x_2 = 1$. M_{w1} is the the weight-average molecular weight of LCPEI, and M_{w2} is the molecular weight of cholesterol.

Table 2 presents two observations on the effect of increasing the hydrophobicity of the LCPEI and increasing the level of cholesterol within the dispersion. On examining N, this value is seen to increase as the number of cetyl chains per molecule or level of cholesterol increased. Vesicle size also increases as the number of cetyl chains per molecule increases and cholesterol causes only modest changes in vesicle size. As cholesterol and the number of cetyl chains increase, so do the hydrophobic forces resulting in a net increase in N as more molecules associate with each other in a given particle.

However, while the addition of more polymer molecules increases vesicle size, the addition of cholesterol increases the intermolecular hydrophobic interactions within the bilayer to produce a denser packing of material in each particle. With cholesterol-containing aggregates, the second virial coefficient becomes less negative as more cholesterol is added to the LCPEI 42 dispersion or as the hydrophobicity of the LCPEI increases in cholesterol-free systems. This indicates that hydrophobic attractions are the dominant forces controlling the self-assembly with a diminished tendency to phase separation arising when an optimum amount of cholesterol is added to the system. On storage for 6 months at room temperature LCPEI 42, cholesterol (2:1 g g^{-1}) vesicles remain colloidally stable (data not shown).

HCPEI, Cholesterol Dispersions. Below a cetylation level of 3 mol %, the membrane stabilizing agent cholesterol resulted in the formation of bilayer vesicles with poor stability (phase separation was observed within 4 h). Cholesterol-containing HCPEI 1 and HCPEI 2 vesicles had a z-average mean hydrodynamic diameter of 400 and 250 nm, respectively. On increasing the level of cetylation to between 3% and 37% (HCPEIs 3, 4, 8, 18, 23, 24, 33, and 37), stable bilayer vesicles were observed (Figure 7a,b).

Cholesterol thus extends the range of amphiphiles that are capable of vesicle formation, and this work provides evidence that molecules with a hydrophobic content of between 12 and 58 wt % are able to form membranes in the presence of cholesterol. Thick unilamellar membranes (of up to 15 nm thick) are observed with these vesicles (Figure7a,b), which we believe is due to the polymer coating which extends beyond the surface

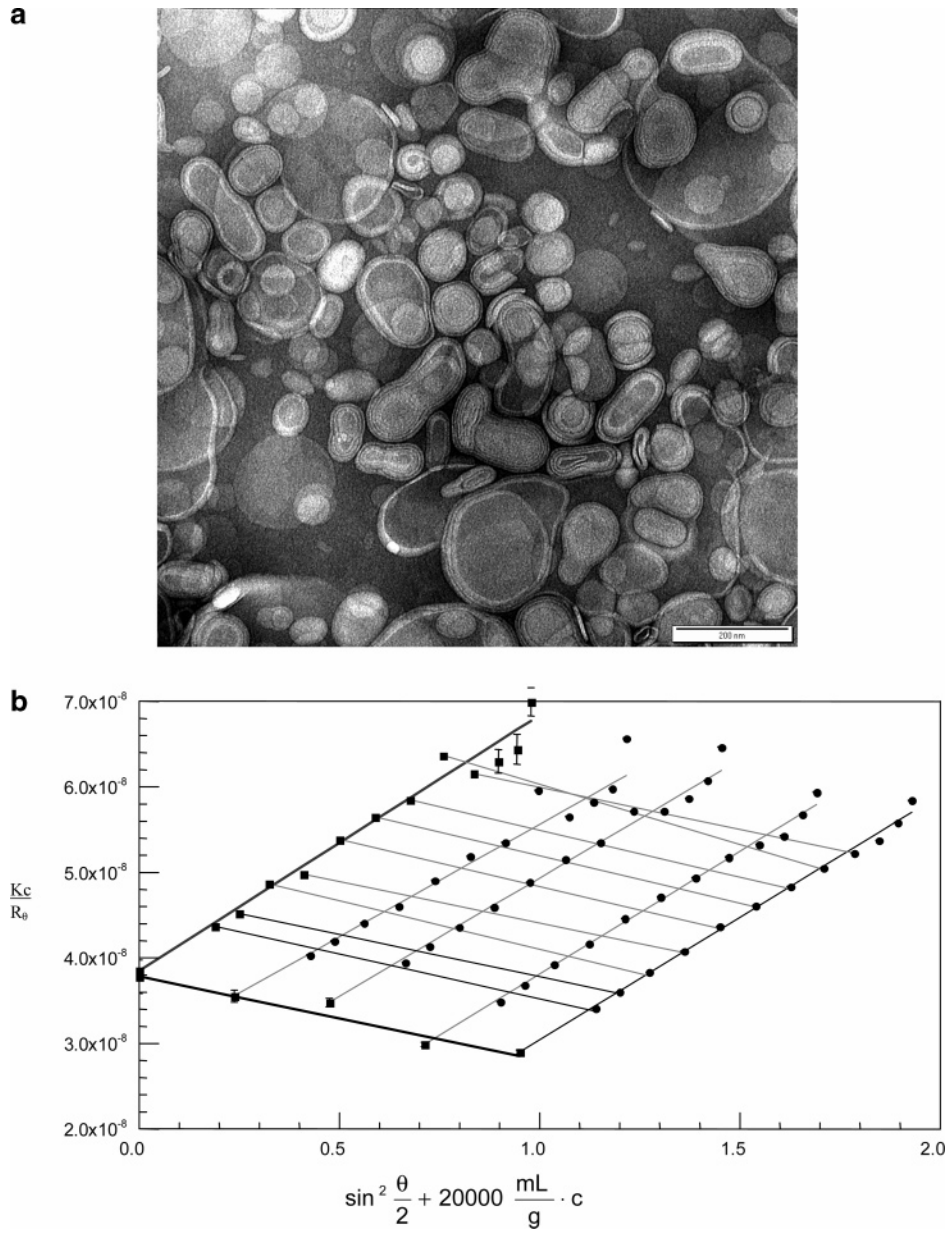

Figure 6. (a) Negative stained TEM of LCPEI 42 (42 mol % cetylation), cholesterol (20 mg mL^{-1}:10 mg mL^{-1}) bilayer vesicles, on probe sonication in water, bar = 200 nm. (b) Zimm plot of LCPEI 42, cholesterol (89:11 g g^{-1}).

Table 2. LCPEI Aggregates[a]

LCPEI (LCPEI, chol molar ratio)	d*n*/d*c* (mL g^{-1})	M_w (kDa)	$A_2 \times 10^4$ (mol mL g^{-2})	R_g (nm)	R_h (nm)	*N*
LCPEI 14, (1.15)	0.171	11 000	−20.68	42	34	11 000
LCPEI 42 (0)	0.157	22 000	−2.814	62	50	16 381
LCPEI 42, (2.3)	0.157	26 000	−17.02	63	51	17 235
LCPEI 42, (1.15)	0.161	34 000	−3.698	65	52	20 332
LCPEI 42, (0.58)	0.163	75 000	−6.637	68	54	37 347

[a] d*n*/d*c* = refractive index increment, M_w = weight-averaged molar mass, A_2 = second virial coefficient, R_g = radius of gyration, R_h = hydrodynamic radius, *N* = number of LCPEI molecules per vesicle.

of the membrane as schematically illustrated in Figure 7b. The HCPEI headgroup occupies a large volume because its polyelectrolyte nature ensures that it enjoys maximum repulsion with its nearest neighbors. The extended polymer coating is a feature of vesicles produced from HCPEIs with a low level of cetylation (Figure 7a,b).

On increasing the level of cetylation to above 37% (HCPEIs 49, 68, and 96), solid nanoparticles which resist the ingress of stain (Figure 7c) are observed. HCPEIs thus form vesicles or amorphous and dense nanoparticle structures depending on the level of cetylation. We can conclude from this work and our earlier work[2,4,24] that once the hydrophobic content of a mol-

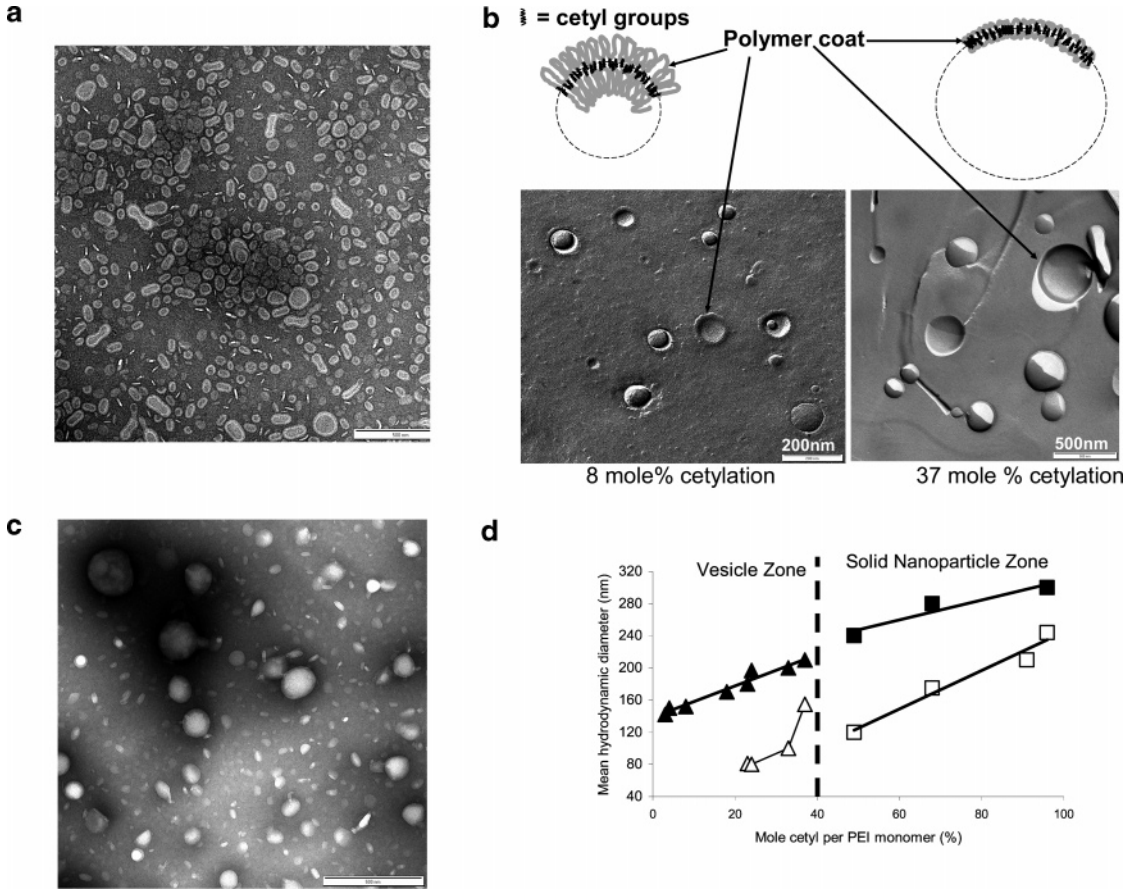

Figure 7. (a) Negative stained TEM of HCPEI 6 (6 mol % cetylation), cholesterol (8 mg mL^{-1}, 4 mg mL^{-1}) vesicles produced by probe sonication in water, bar = 500 nm. Vesicles consist of a lipid bilayer (resists staining), stained polymer coat, and stained interior. (b) A high level of cetylation leads to a larger vesicle size. Polymer coat is visible with low levels of cetylation. With higher levels of cetylation less of the polyelectrolyte portion of the polymer will be available to form a polymer coat, and more of the polymer will have intimate contact with the lipid portion of the bilayer. Cholesterol moieties have been omitted for clarity. Vesicles were prepared by the probe sonication of HCPEI 8 (8 mol % cetylation) or HCPEI 37 (37 mol % cetylation) at a concentration of 4 mg mL^{-1} together with cholesterol at a concentration of 2 mg mL^{-1}. (c) Negative stained TEM of HCPEI 49 (49% cetylation), cholesterol (4 mg mL^{-1}:2 mg mL^{-1}) nanoparticles prepared by probe sonication in water, bar = 500 nm. (d) Effect of hydrophobicity on aggregate size. ▲, △ = vesicles; ■, □ = nanoparticles; closed symbols = aggregates prepared with cholesterol (HCPEI, cholesterol = 2:1 weight ratio); open symbols = aggregates prepared in the absence of cholesterol.

ecule exceeds a critical value, membrane formation is prevented even in the presence of the membrane stabilizing agent, cholesterol. This may have important implications for the formation of biological colloids or deposits.

Particle Size. A further striking feature of these particles is the linear effect of cetylation on particle hydrodynamic diameter (Figure 7d and eqs 6−8)

$$D_{vc} = 1.95Ct + 139 \; (r = 0.98) \tag{6}$$

$$D_{n} = 2.31Ct + 5.55 \; (r = 0.98) \tag{7}$$

$$D_{nc} = 1.26Ct + 185 \; (r = 0.96) \tag{8}$$

where Ct = mol % cetylation and D_{vc}, D_{n}, and D_{nc} are the mean hydrodynamic diameter of HCPEI−cholesterol vesicles, HCPEI solid nanoparticles, and HCPEI−cholesterol nanoparticles, respectively. The reduced radius of curvature with these polymeric amphiphiles on increase in cetyl content is illustrated schematically in Figure 7b. With the LCPEIs, an increase in cetylation led to an increase in the aggregation number and vesicle size. We thus conclude that as the hydrophobicity of the polymers increases or cholesterol is added (Figure 7d), more molecules are involved in the formation of each aggregate in order to effectively shield their hydrophobic moieties from energetically unfavorable contact with the aqueous phase, and an increase in vesicle size is seen. With the LCPEIs, the increase in size on addition of cholesterol is more modest (Table 2).

The last feature to note is that as the size of molecule increases the size of the aggregate increases (e.g., Figure 5b compared to Figure 7b). Larger molecules are known to have a smaller radius of curvature.[3]

Conclusions

In the present work key drivers for the self-assembly of macromolecules into colloidal dispersions have been elucidated. Hydrophobic interactions are crucial for the formation of membranes, enhancing these interactions by the incorporation of cholesterol within the assemblies enhances membrane formation. Amphiphiles must have between 12 and 58% hydrophobic content in order to form membranes in the presence of cholesterol and between 43 and 58% hydrophobic content for membrane formation in the absence of cholesterol. Micellization occurs when the hydrophobic content is below 43%. Cholesterol and amphiphile hydrophobic content increase the aggregation number of molecules in the colloidal particles, and also the particle size and a linear relationship exists between % cetylation and mean

particle size. The heterogeneity within the substituted polymers leads to a variety of unusual morphologies such as tubular micelles and flattened vesicles as polymers within each synthetic batch consist of heavily substituted (hydrophobic) and lightly substituted (hydrophilic) molecules which are able to stabilize the various sections of the particles. Finally, larger sized molecules form larger colloidal particles, and d*n*/d*c* measurements are an accurate estimation of the hydrophobic content of a macromolecule. Apart from the obvious implications for the fabrication of various nanomaterials, this work may also have implications for the structural contributions played by endogenous macromolecules such as glcycoproteins and lipoproteins in membranes and biological colloids.

References and Notes

(1) Lee, A. G. *Biochim. Biophys. Acta* **2003**, *1612*, 1−40.
(2) Wang, W.; Tetley, L.; Uchegbu, I. F. *Langmuir* **2000**, *16*, 7859−7866.
(3) Wang, W.; McConaghy, A. M.; Tetley, L.; Uchegbu, I. F. *Langmuir* **2001**, *17*, 631−636.
(4) Wang, W.; Tetley, L.; Uchegbu, I. F. *J. Colloid Interface Sci.* **2001**, *237*, 200−207.
(5) Goula, D.; Benoist, C.; Mantero, S.; Merlo, G.; Levi, G.; Demeneix, B. A. *Gene Ther.* **1998**, *5*, 1291−1295.
(6) Furgeson, D. Y.; Chan, W. S.; Yockman, J. W.; Kim, S. W. *Bioconjugate Chem.* **2003**, *14*, 840−847.
(7) Han, S. O.; Mahato, R. I.; Kim, S. W. *Bioconjugate Chem.* **2001**, *12*, 337−345.
(8) Ferguson, D. Y.; Cohen, R. N.; Mahato, R. I.; Kim, S. W. *Pharm. Res.* **2002**, *19*, 382−390.
(9) Klotz, I. M.; Royer, G. P.; Sloniewsky, A. R. *Biochemistry* **1969**, *8*, 4752−4756.
(10) Khmelnitsky, Y. L.; Gladilin, A. K.; Roubailo, V. L.; Martinek, K.; Levashov, A. V. *Eur. J. Biochem.* **1992**, *206*, 737−745.
(11) Noding, G.; Heitz, W. *Macromol. Chem. Phys.* **1998**, *199*, 1637−1644.
(12) Wang, D.; Narang, A. S.; Kotb, M.; Gaber, A. O.; Miller, D. D.; Kim, S. W.; Mahato, R. I. *Biomacromolecules* **2002**, *3*, 1197−1207.
(13) Kim, S.; Choi, J. S.; Jang, H. S.; Suh, H.; Park, J. *Bull. Korean Chem. Soc.* **2001**, *22*, 1069−1075.
(14) Oku, N.; Shibamoto, S.; Ito, F.; Gondo, H.; Nango, M. *Biochemistry* **1987**, *26*, 8145−8150.
(15) Zimm, B. H. *J. Chem. Phys.* **1948**, *16*, 1093.
(16) Zimm, B. H. *J. Chem. Phys.* **1948**, *16*, 1099−1116.
(17) Pecora, R. *Dynamic Light Scattering: Applications of Photon Correlation Spectroscopy;* Plenum Press: New York, 1985.
(18) Uchegbu, I. F.; Schatzlein, A. G.; Tetley, L.; Gray, A. I.; Sludden, J.; Siddique, S.; Mosha, E. *J. Pharm. Pharmacol.* **1998**, *50*, 453−8.
(19) Sorlier, P.; Rochas, C.; Morfin, I.; Vilton, C.; Domard, A. *Biomacromolecules* **2003**, *4*, 1034−1040.
(20) Zhu, D. M.; Wu, X.; Schelly, Z. A. *J. Phys. Chem.* **1992**, *96*, 7121−7126.
(21) Uchegbu, I. F.; Sadiq, L.; Arastoo, M.; Gray, A. I.; Wang, W.; Waigh, R. D.; Schätzlein, A. G. *Int. J. Pharm.* **2001**, *224*, 185−199.
(22) Uchegbu, I. F.; Florence, A. T. *Adv. Colloid Interface Sci.* **1995**, *58*, 1−55.
(23) New, R. R. C. *Liposomes: A Practical Approach;* Practical Approach Series; Oxford University Press: Oxford, 1990.
(24) Uchegbu, I. F.; Tetley, L.; Wang, W. Nanoparticles and Polymeric Vesicles from New Poly-L-lysine Based Amphiphiles. In *Biomaterials for Drug Delivery and Tissue Engineering*; Mallapragada, S., et al., Eds.; Materials Research Society: Warrendale, PA, 2001; pp NN6.8.1−NN6.8.6.

MA049042O